

Phenomenology of a nonstandard Higgs boson in $W_L W_L$ scattering

Vassilis Koulovassilopoulos* and R. Sekhar Chivukula†

Physics Department, Boston University, 590 Commonwealth Avenue, Boston, Massachusetts 02215

(Received 13 April 1994)

In this paper we consider the phenomenology of a nonstandard Higgs boson in longitudinal gauge boson scattering. First, we present a composite Higgs model [based on an $SU(4)/Sp(4)$ chiral-symmetry breaking pattern] in which there is a nonstandard Higgs boson. Then we explore, in a model-independent way, the phenomenology of such a nonstandard Higgs boson by calculating the leading one-loop logarithmic corrections to longitudinal gauge boson scattering. This calculation is done using the equivalence theorem and the Higgs boson is treated as a scalar-isoscalar resonance coupled to the Goldstone bosons of the $SU(2)_L \times SU(2)_R / SU(2)_V$ chiral symmetry breaking. We show that the most important deviation from the one-Higgs-doublet standard model is parametrized by one unknown coefficient which is related to the Higgs-boson width. The implications for future hadron colliders are discussed.

PACS number(s): 14.80.Cp, 12.60.Fr, 12.60.Rc, 13.85.Qk

I. INTRODUCTION

Although it is well established that the electroweak interactions are described by a spontaneously broken $SU(2) \times U(1)$ gauge theory, the underlying physics of the symmetry breaking is still elusive. In the minimal (one-Higgs-doublet) standard model (SM), electroweak symmetry breaking is assumed to be due to an $SU(2)_L \times SU(2)_R$ Gell-Mann–Levy linear σ model. In the broken phase this theory has a neutral scalar particle, the Higgs boson (H), which, along with the isotriplet (w^a) of Goldstone bosons of the spontaneously broken $SU(2)_L \times SU(2)_R$ symmetry (which become the longitudinal components of the W^\pm and Z) completes a complex scalar doublet. The σ -model dynamics provide the Higgs boson a mass which is proportional to the quartic self-coupling λ , and is unconstrained by any symmetry. If the Higgs boson is heavy, the model becomes strongly coupled, and perturbation theory breaks down [1,2].

However, there are good reasons to believe that no scalar field theory can be fundamental. First, scalar field theories are “unnatural” [3]: since no (ordinary) symmetry protects scalar masses, theories without supersymmetry require a large amount of fine tuning to maintain a hierarchy between the weak scale and any higher scale in the theory. There is, however, a strong restriction on such theories coming from the analysis of their short-distance behavior. Consideration of the dynamics seems to suggest that scalar field theories are trivial in the continuum limit [4,5]: for a physically meaningful bare coupling (λ_0) the renormalized coupling (λ_R) is forced to be zero in the limit that the cutoff (Λ) is sent to infinity. As the cutoff decreases, the upper bound on λ_R , and, consequently, on the Higgs-boson mass $m_H = 2\lambda_R v^2$, increases. Of course,

in order that the theory makes sense, m_H must be less than Λ . This sets a maximum upper bound, which is estimated to be roughly 600–800 GeV, if Λ is of order a few TeV [6]. This suggests that the standard model can only be viewed as low-energy effective theory below some scale Λ where additional new physics enters.

Physically, it is more relevant to interpret the triviality bound by turning the argument around: if the electroweak symmetry breaking (EWSB) sector involves a heavy (iso)scalar resonance that couples to the electroweak gauge bosons, then one should expect that it has properties rather differ from those of the SM Higgs boson and that these deviations become larger as the mass of this putative Higgs boson grows. Such a particle we generically call a “nonstandard Higgs boson.” With luck, the physics of symmetry breaking will be directly probed [7] in the next generation of high-energy colliders [e.g., the CERN Large Hadron Collider (LHC)], perhaps through longitudinal gauge boson scattering [8].

In this paper we will compute the leading one-loop corrections to longitudinal gauge boson scattering in a theory with a nonstandard Higgs boson. At sufficiently high energy, using the equivalence theorem [2,9,10], the (strong) scattering amplitudes of the Goldstone bosons which would be present in the absence of the electroweak gauge symmetry are approximately the same as those of the longitudinal electroweak gauge bosons. The interactions of Goldstone bosons are conveniently described in the language of chiral Lagrangians [11–13]. To lowest order in momentum, the most general effective theory that contains an isoscalar “Higgs” boson and the isotriplet of Goldstone bosons of the spontaneously broken $SU(2)_L \times SU(2)_R$ symmetry (at energies below the cutoff scale Λ) [11,14] is

$$\mathcal{L} = \frac{1}{4} \left(v^2 + 2\xi v H + \xi' H^2 + \xi'' \frac{H^3}{6v} \right) \text{Tr}(\partial_\mu U^\dagger \partial^\mu U) + \mathcal{L}_H, \quad (1)$$

*Electronic address: vk@budo.e.bu.edu

†Electronic address: sekhar@abel.bu.edu

where ξ , ξ' , and ξ'' are unknown coefficients, $v=246$ GeV, and U contains the Goldstone bosons w^a

$$U = \exp\left(\frac{i\mathbf{w} \cdot \boldsymbol{\tau}}{v}\right), \quad \text{Tr}(\tau^a \tau^b) = 2\delta^{ab}, \quad (2)$$

where $\boldsymbol{\tau}$ the Pauli matrices and \mathcal{L}_H the Lagrangian for the isoscalar

$$\mathcal{L}_H = \frac{1}{2}(\partial_\mu H)^2 - \frac{m^2}{2}H^2 - \frac{\lambda_3 v}{3!}H^3 - \frac{\lambda_4}{4!}H^4. \quad (3)$$

Here $SU_L(2)$ corresponds to $SU(2)_{\text{weak}}$, while the τ_3 component of the custodial $SU(2)_R$ corresponds to hypercharge. In addition, for simplicity, we have included only the leading nonderivative terms in the scalar potential (which are the only ones relevant for this investigation). The ordinary linear σ model corresponds to the limit

$$\xi, \xi' = 1, \quad \xi'' = 0 \quad (4)$$

and

$$\lambda_3, \lambda_4 = \frac{3m^2}{v^2}. \quad (5)$$

In the next section, we will illustrate the possibility of a nonstandard Higgs boson by constructing a composite Higgs model of the Georgi-Kaplan type [15,16] based on an $SU(4)/\text{Sp}(4)$ symmetry breaking pattern. Here the compositeness scale will be identified with the cutoff Λ of the composite Higgs effective theory. In the limit that $\Lambda \rightarrow \infty$, any composite Higgs model reduces to the standard model. However, if the Higgs boson is heavy, new physics must enter at a scalar of the order of a few TeV, and deviations from the standard model may be large [14]. For this example, we derive the relationship between the parameters of the composite Higgs theory and the parameters in the Lagrangian Eq. (1) above.

In Sec. III, we present the calculation of the one-loop corrections to longitudinal gauge boson scattering in a model-independent manner by starting from the general effective theory of Eq. (1). Section III elaborates on the results presented in [14]. Sections II and III are essentially independent of one another.

Section IV contains our conclusions. Finally, Appendix A contains an explicit form of the Lagrangian for the $SU(4)/\text{Sp}(4)$ model, Appendix B contains the Feynman rules for the Lagrangian (1), and Appendix C the analytical expressions for the one-loop integrals used in Sec. III.

II. THE $SU(4)/\text{Sp}(4)$ MODEL

In this section we shall describe an explicit model which contains a nonstandard Higgs boson. We focus here only on the phenomenology of the longitudinal gauge boson scattering. The ordinary fermions will not enter our analysis and, therefore, we neglect the issue of ordinary fermion mass generation (though it is straightforward to extend the model to generate fermion masses).

The model assumes the existence of a new strong and confining ‘‘ultracolor’’ interaction based on the gauge

group G_c , four new left-handed *ultrafermions* transforming in a pseudoreal representation of G_c (recall that there must be an even number of fermions in order to avoid the Witten anomaly [17]), and a fundamental scalar doublet. The presence of a fundamental scalar doublet is somewhat unsatisfactory. However, as we will see, the mass of the nonstandard Higgs boson in this model can be as large as 700 GeV without the self-interactions of the fundamental scalar doublet being particularly strong: in this sense the theory is *less trivial* than the usual fundamental scalar-doublet standard model with a heavy Higgs boson.

In the limit that the ultrafermions are massless and the limit of vanishing Yukawa coupling between the fermions and the fundamental scalar, the global chiral symmetry of the ultrafermions is $G=\text{SU}(4)$. These fermions have electroweak quantum numbers: one $SU(2)_W$ doublet with hypercharge $Y=0$ and two $SU(2)_W$ singlets with $Y = \pm \frac{1}{2}$. The explicit form of the $SU(2)_W \times U(1)_Y$ generators embedded in the flavor group G is given by

$$\mathbf{S} = \frac{1}{2} \begin{pmatrix} \boldsymbol{\tau} & 0 \\ 0 & 0 \end{pmatrix}, \quad Y = \frac{1}{2} \begin{pmatrix} 0 & 0 \\ 0 & \tau_3 \end{pmatrix}, \quad (6)$$

where $\boldsymbol{\tau}$ are the Pauli matrices and as usual the electromagnetic charge is generated by $Q = S_3 + Y$.

When the ultracolor interactions G_c become strong, at the ‘‘chiral symmetry breaking’’ scale Λ (which will be on the order of a TeV or higher), a condensate is produced,

$$\langle \psi \psi^T \rangle \approx \Lambda f^2 \Delta, \quad (7)$$

where T denotes the transpose in ultracolor space, f is the ‘‘ f constant’’ for ultracolor chiral symmetry breaking (the analog of $f_\pi=93$ MeV in QCD), and Δ is a unitary matrix in flavor space that characterizes the vacuum orientation. The rules of ‘‘naive dimensional analysis’’ [12] imply that Λ must be less than or of order $4\pi f$.

By making a G transformation, Δ can be brought to the form

$$\Delta = \begin{pmatrix} \tau_2 & 0 \\ 0 & \tau_2 \end{pmatrix}. \quad (8)$$

The condensate (7) spontaneously breaks the chiral symmetry G down to the subgroup $H=\text{Sp}(4)$ [18–20], producing five Goldstone bosons (which would be massless in the absence of electroweak gauge interactions, and the Yukawa couplings and fermion mass terms described below). Notice that $SU(2)_W \times U(1)_Y$ is contained in $H=\text{Sp}(4)$ and thus is not broken at the scale Λ by the ultrafermion condensate. Furthermore, electroweak radiative corrections will not induce such a breaking [18]. As we show in the Sec. II A, the Yukawa couplings to the fundamental scalar will be responsible for misaligning the vacuum slightly and driving electroweak symmetry breaking.

The ten unbroken $\text{Sp}(4)$ generators \mathcal{N}^i and the broken ones \mathcal{X}^a satisfy the relations¹

¹The first relation follows from the definition of the $\text{Sp}(4)$ algebra.

$$\Delta \mathcal{N}^\top \Delta = -\mathcal{N}, \quad \Delta \mathcal{X}^\top \Delta = \mathcal{X}. \quad (9)$$

The broken generators \mathcal{X}^a , conveniently normalized as $\text{Tr}(\mathcal{X}^a \mathcal{X}^b) = \frac{1}{2} \delta^{ab}$, are given by

$$X = \frac{1}{2\sqrt{2}} \begin{pmatrix} 0 & I \\ I & 0 \end{pmatrix}, \quad \mathbf{T} = \frac{1}{2\sqrt{2}} \begin{pmatrix} 0 & -\tau \\ \tau & 0 \end{pmatrix}, \quad (10)$$

$$A = \frac{1}{2\sqrt{2}} \begin{pmatrix} I & 0 \\ 0 & -I \end{pmatrix}.$$

The algebra of $\text{Sp}(4)$ is isomorphic to that of $\text{SO}(5)$, which contains an $\text{SO}(4) \simeq \text{SU}(2) \times \text{SU}(2)$ subgroup given by Eq. (6), with Y being the third component of the custodial $\text{SU}(2)$ symmetry. Thus the five Goldstone bosons $\Pi^\alpha = (\sigma, \boldsymbol{\pi}, a)$, $\alpha = 1, \dots, 5$, fall into a representation which decomposes under $\text{SU}(2) \times \text{SU}(2)$ as the sum of a $(\mathbf{2}, \mathbf{2})$

$$\Phi = \sigma X + i\boldsymbol{\pi} \cdot \mathbf{T} \quad (11)$$

that has the quantum numbers of the usual Higgs doublet, and a $(\mathbf{1}, \mathbf{1})$, the a , that appears as an electroweak singlet. For convenience we will denote the complex doublet of fundamental scalars Φ' , which also transforms under $\text{SU}(2)_L \times \text{SU}(2)_R$ as $(\mathbf{2}, \mathbf{2})$, by

$$\Phi' = \sigma' X + i\boldsymbol{\pi}' \cdot \mathbf{T}. \quad (12)$$

Below the chiral symmetry breaking scale Λ , the dynamics of the Goldstone bosons can be described by an effective chiral Lagrangian, in analogy with QCD [11–13]. Using a nonlinear realization, the Π^α are incorporated into the field ξ

$$\xi = \exp\left(\frac{i\Pi^\alpha \mathcal{X}^\alpha}{f}\right), \quad \xi \rightarrow \xi' = g\xi h^\dagger, \quad (13)$$

where $g \in G$, $h \in H$. As usual, it is more convenient to define the field $\Sigma = \xi^2$, which transforms linearly under H . By using Eq. (9) and noting that $\xi^2 = \xi \Delta \xi^\top \Delta$, it is easy to show that Σ transforms under G like

$$\Sigma \rightarrow g\Sigma g^\dagger, \quad g \in H \quad (14)$$

$$\Sigma \rightarrow g\Sigma g, \quad g \in G/H.$$

The interactions of the Π with the $\text{SU}(2)_W \times \text{U}(1)_Y$ gauge bosons are described to lowest order in momentum by a gauged G/H nonlinear σ model

$$\mathcal{L}_\Sigma = \frac{f^2}{4} \text{Tr}(D_\mu \Sigma^\dagger D^\mu \Sigma) + \frac{M^2 f^2}{2} \text{Tr}(\Sigma + \Sigma^\dagger) \quad (15)$$

with the covariant derivative defined as

$$D_\mu \Sigma = \partial_\mu \Sigma + ig[\mathbf{S}, \Sigma] \cdot \mathbf{W}_\mu + ig'[Y, \Sigma] \mathcal{B}_\mu. \quad (16)$$

In the second term in Eq. (15) we have assumed that the Π^α have a mass due to a G_c and $\text{SU}(2)_W \times \text{U}(1)_Y$ invariant mass term for the ultrafermions. In the fundamental theory, this fermion mass term is of the form

$\mathcal{M} \psi^\top \Delta \psi$. In the low-energy theory $M^2 = \mu \mathcal{M}$, where μ is a dimensionful constant of order Λ .

The interactions of the fundamental scalar Φ' are described by the usual ϕ^4 Lagrangian, given by

$$\mathcal{L}_\phi = \text{Tr}(D_\mu \Phi'^\dagger D^\mu \Phi') - \lambda \left(\text{Tr}(\Phi'^\dagger \Phi') + \frac{m_\phi^2}{2\lambda} \right)^2. \quad (17)$$

Here $m_\phi^2 > 0$, so that the electroweak symmetry is not broken through the interactions in Eq. (17) alone.

Finally, Φ' and Π mix through Yukawa couplings of Φ' with the ultrafermions ψ^i . Above the chiral symmetry breaking scale Λ this interaction is of the form $iy\psi^\top \Delta \Phi' \psi$ plus H.C. In the effective theory, to lowest order in y , it becomes an interaction between Φ' and Π given by

$$\mathcal{L}_{\text{Yuk}} = \frac{iy\mu f^2}{2} \text{Tr} \Phi' (\Sigma^\dagger - \Sigma). \quad (18)$$

Notice that in Eq. (18) we have included only pseudoscalar couplings. In principle we could also have scalar couplings, but for the vacuum to align so as to break the electroweak symmetry it is essential that there are nonzero pseudoscalar couplings. The addition of scalar couplings of the fundamental doublet would not qualitatively change the analysis.

Now we can gather all the pieces together to write the Lagrangian \mathcal{L}_{eff} of the $\text{SU}(4)/\text{Sp}(4)$ model for scales below Λ . To lowest order in momentum and the other symmetry breaking terms (M and y), it is given by

$$\mathcal{L}_{\text{eff}} = \mathcal{L}_\Sigma + \mathcal{L}_\phi + \mathcal{L}_{\text{Yuk}}. \quad (19)$$

A. Vacuum alignment

Let us now examine the ground state of the Lagrangian in Eq. (19). Since we do not want to break electromagnetism, we search for a minimum of the potential of our effective theory with expectation values only for the two isosinglets (σ, σ') . (All other vacua which preserve electromagnetism are equivalent to these up to a chiral rotation.) Setting $\boldsymbol{\pi} = \boldsymbol{\pi}' = a=0$, the potential is given by

$$V(\sigma, \sigma') = \frac{m_\phi^2}{2} \sigma'^2 + \frac{\lambda}{4} \sigma'^4 - 4M^2 f^2 \cos\left(\frac{\sigma}{\sqrt{2}f}\right) - \sqrt{2}\mu f^2 y \sigma' \sin\left(\frac{\sigma}{\sqrt{2}f}\right). \quad (20)$$

The conditions $\partial V/\partial \sigma = 0$ and $\partial V/\partial \sigma' = 0$, which determine the extrema, always have the trivial solution $\sigma = \sigma' = 0$, for arbitrary values of the couplings. However, a solution exists for nonzero values of σ and σ' if

$$\frac{y f \mu}{\sqrt{2} M m_\phi} > 1, \quad m_\phi > 0 \quad (21)$$

and this solution has lower energy than $\sigma = \sigma' = 0$. That is, for $y > y_c = \sqrt{2} M m_\phi / \mu f$ the vacuum becomes unstable, giving vacuum expectation values (VEV's) to both σ and σ' , and thereby breaking $\text{SU}(2)_W \times \text{U}(1)_Y$. One com-

bination of the π and π' becomes the longitudinal components of W^\pm and Z , while the orthogonal combinations remain in the spectrum as a degenerate (due to isospin) pseudoscalar isotriplet. Expanding Eqs. (15),(17) and requiring that the W and Z masses be correct, we obtain

$$v^2 = 2f^2 \sin^2 \frac{\langle \sigma \rangle}{\sqrt{2}f} + \langle \sigma' \rangle^2, \quad (22)$$

where $v=246$ GeV.

It is convenient to recast our description in the more familiar notation of the two-Higgs-doublet model by defining

$$\begin{aligned} \sqrt{2}f \sin \frac{\langle \sigma \rangle}{\sqrt{2}f} &= v \cos \alpha, \\ \langle \sigma' \rangle &= v \sin \alpha. \end{aligned} \quad (23)$$

In order to identify the mass eigenstate fields, we perform a field redefinition in \mathcal{L}_{eff} and rewrite Σ and Φ' as

$$\Sigma = \mathcal{U}^\dagger \Sigma_0 \mathcal{U}, \quad \Phi' = \mathcal{V}^\dagger \Phi'_0 \mathcal{V} \quad (24)$$

where

$$\mathcal{U} = \exp \left(\frac{2i\mathbf{S} \cdot \boldsymbol{\pi}}{v \cos \alpha} \right), \quad \mathcal{V} = \exp \left(\frac{2i\mathbf{S} \cdot \boldsymbol{\pi}'}{v \sin \alpha} \right) \quad (25)$$

and

$$\begin{aligned} \Sigma_0 &= \exp \left(\frac{2iX}{f} (\sigma + \langle \sigma \rangle) \right), \\ \Phi'_0 &= (\sigma' + \langle \sigma' \rangle) X, \end{aligned} \quad (26)$$

where for simplicity σ and σ' denote now the shifted fields. This field redefinition leaves all S -matrix elements invariant [21], and the resulting Lagrangian obtained after some straightforward but tedious algebra is provided in Eq. (A2) in Appendix A.

It is now straightforward to identify the mass eigenstates \mathbf{w} and \mathbf{p} as those obtained from $\boldsymbol{\pi}$ and $\boldsymbol{\pi}'$ by making a rotation by α ,

$$\begin{pmatrix} \mathbf{w} \\ \mathbf{p} \end{pmatrix} = \begin{pmatrix} \cos \alpha & \sin \alpha \\ -\sin \alpha & \cos \alpha \end{pmatrix} \begin{pmatrix} \boldsymbol{\pi} \\ \boldsymbol{\pi}' \end{pmatrix}. \quad (27)$$

The \mathbf{w} correspond to the exact Goldstone bosons that are “eaten” by the longitudinal states of W_a^μ , while \mathbf{p} remains in the spectrum as a degenerate massive isotriplet.

The 2×2 mass-squared matrix for the two neutral (isosinglet) scalar states σ and σ' , defined by

$$\left. \frac{\partial^2 V}{\partial \sigma_i \partial \sigma_j} \right|_{\sigma=0}, \quad (28)$$

is obtained from Eq. (20) by using Eqs. (22) and (23). Its explicit form is given by

$$y\mu f \begin{pmatrix} \tan \alpha & -\sqrt{1 - \frac{v^2 \cos^2 \alpha}{2f^2}} \\ -\sqrt{1 - \frac{v^2 \cos^2 \alpha}{2f^2}} & \frac{1}{\tan \alpha} + \frac{2\lambda v^2 \sin^2 \alpha}{yf\mu} \end{pmatrix}. \quad (29)$$

The eigenstates of this symmetric matrix correspond to the isosinglet mass eigenstates H, h and are found by performing a rotation² on σ and σ' ,

$$\begin{pmatrix} H \\ h \end{pmatrix} = \begin{pmatrix} \cos \beta & \sin \beta \\ -\sin \beta & \cos \beta \end{pmatrix} \begin{pmatrix} \sigma \\ \sigma' \end{pmatrix}. \quad (30)$$

The expressions for the masses m, m_h of H and h , respectively, as well as the angle β are not particularly illuminating except in some limiting cases that we discuss below.

Two ranges of the parameters are of particular interest: (i) Having $f \gg v$ and small Yukawa coupling and (ii) having f of $O(v)$ and Yukawa coupling $y \simeq 1$. In the first case, by taking the scale $f \gg v$ we find that $\alpha - \beta \sim O(v^2/f^2)$. The masses of the heavy Higgs boson h , the massive isotriplet \mathbf{p} , and the singlet a , grow with f , with the h and \mathbf{p} becoming degenerate. All of these states decouple from light states H, w^a in the usual sense of Appelquist and Carazzone [22]. On the other hand, the mass of the “light” Higgs boson, m , does not grow with f . Setting $\mu \approx 4\pi f$, in the $f \rightarrow \infty$ limit m tends to

$$m^2 \rightarrow 2(\lambda \sin^4 \alpha + \pi y \sin \alpha \cos^3 \alpha) v^2. \quad (31)$$

In this limit³ the $SU(4)/Sp(4)$ model reduces exactly to the standard model in the spontaneously broken phase written in “polar” coordinates

$$\sigma + v + i\boldsymbol{\tau} \cdot \boldsymbol{\pi} \equiv (H + v) \exp \left(\frac{i\mathbf{w} \cdot \boldsymbol{\tau}}{v} \right),$$

with the value of the λ_{ϕ^4} coupling renormalized at scale Λ equal to $\lambda \sin^4 \alpha + \pi y \sin \alpha \cos^3 \alpha$.

Case (ii), where $f \simeq O(v)$, however, is more interesting since it is the regime where the “light” scalar Higgs is entirely “nonstandard.” In order to give an idea of this regime, we take as reference the values

$$f = 180 \text{ GeV}, \quad \lambda = 1, \quad \alpha = 30^\circ, \quad y = 3.5. \quad (32)$$

For these values the mass spectrum is

$$m = 718 \text{ GeV}, \quad m_h = 1675 \text{ GeV}, \quad m_p = 1814 \text{ GeV}, \quad (33)$$

$$m_a = 907 \text{ GeV}, \quad \beta = 21.5^\circ, \quad \Lambda \approx 4\pi f \simeq 2.2 \text{ TeV}.$$

As advertised, the Higgs mass is of order 700 GeV without the self-coupling of the fundamental scalar being particularly large. The Lagrangian Eq. (19) does include only the *lowest order* terms in the effective chiral theory. However, using the rules of dimensional analysis [12] we see that, for the values chosen in Eq. (32), the higher order terms should not significantly change the vacuum structure of the theory [15].

²In the literature of the two-Higgs-doublet models the angles α and β are sometimes defined the other way around, namely, α rotating the isosinglet states and β rotating the isotriplets.

³Of course this limit requires a large amount of fine tuning in order to maintain the hierarchy between f and v .

For generic values of the parameters this model has a mass gap⁴ between the lowest lying states H, w^a and the other heavy particles h, p^a, a . Hence it is reasonable to focus on the interactions of the light scalars. “Integrating out” the heavy states, the $SU(4)/Sp(4)$ theory has precisely the form proposed in Eq. (1), in terms of a single isoscalar resonance with the values of $\xi, \xi', \xi'', \lambda_3, \lambda_4$ given as a functions of f, λ, α, y in Appendix A. Generically we have

$$\xi, \xi' = 1 + O\left(\frac{v^2}{f^2}\right), \quad \xi'' = O\left(\frac{v^2}{f^2}\right) \quad (34)$$

and

$$\lambda_3, \lambda_4 = \frac{3m^2}{v^2} + O\left(\frac{v^2}{f^2}\right). \quad (35)$$

In particular, for the reference values in Eq. (32)

$$\begin{aligned} \xi = 0.62, \quad \xi' = -0.21, \quad \xi'' = 0.71, \\ \lambda_3 = 18.26, \quad \lambda_4 = 4.79. \end{aligned} \quad (36)$$

III. LONGITUDINAL GAUGE BOSON SCATTERING

Using the equivalence theorem [2,9,10], high-energy $W_L W_L$ scattering amplitudes in the full gauge theory can be reliably computed purely in the scalar sector by replacing the longitudinal components of the gauge bosons with the corresponding Goldstone boson. In this section, we will analyze the Lagrangian in Eq. (1) which describes, to lowest order in momentum, the most general theory with a massive scalar-isoscalar resonance coupled to the isotriplet of exact Goldstone bosons of the $SU(2)_L \times SU(2)_R$ symmetry spontaneously broken down to $SU(2)_{L+R}$. In particular, we explore the consequences of such a “nonstandard Higgs” boson for longitudinal gauge boson scattering. The discussion given here completes the analysis begun in Ref. [14].

Chiral perturbation theory [12,13,23] has been used extensively to study the phenomenology of gauge boson scattering, but generally under the assumption that the *only*⁵ strongly interacting degrees of freedom lighter than a TeV were the longitudinal gauge bosons themselves [25–27]. If there were a Higgs boson as heavy as a TeV, then for energies lower than that it would be sufficient to

“integrate out” the Higgs and estimate its effects at lower energies on the processes involving only W^\pm, Z [27,28]. However, here the Higgs resonance is light enough compared to the cutoff Λ or the other heavy resonances in the model, so we must include it explicitly in the effective Lagrangian. Note that, in this limit, the theory is *very* different than QCD, in which there is no significant mass gap between the lightest resonance and any of the others.

In this theory, we present a calculation of the leading one-loop corrections to longitudinal gauge boson scattering $w^+ w^- \rightarrow zz$. (All other channels can be obtained from this one by crossing.) The treatment of infinities induced by loops follows the standard rules of effective nonrenormalizable theories [12,23]. Namely, the infinities associated with nonderivative interactions in the Lagrangian Eq. (1) are absorbed in the renormalization of the scalar self-couplings, while those associated with vertices involving derivatives are absorbed in $SU(2)_L \times SU(2)_R$ invariant counterterms which are of order p^4 . The coefficients of these counterterms are new independent (running) couplings in the theory and cannot be computed. In what follows, we shall compute the leading corrections in the modified minimal subtraction (\overline{MS}) scheme, setting the higher order counterterms to zero when the renormalization scale μ is taken to be $\Lambda \simeq 4\pi f$. These results include the so-called “chiral logarithms” of the pure Goldstone boson theory, which are the largest contributions at sufficiently low momentum [29,30]. As required by consistency of the chiral expansion [12,13], these corrections are expected to be comparable in magnitude to the p^4 counterterms and should provide a reasonable estimate of the size of higher order effects.

In addition, in our computation we have kept the “finite” parts of $O(p^4)$ terms that come along with the logarithms in the \overline{MS} scheme. Unlike the chiral logarithms, these corrections are scheme dependent; therefore, in general, they have no physical meaning. However, in the limit $f \rightarrow \infty$ the theory reduces to the one-Higgs-doublet standard model and, as in any renormalizable theory, all of the μ dependence of our answers should disappear. In this limit we should recover the exact one-loop amplitude for the linear sigma model provided in Ref. [31]. This will serve as an important check for our calculation.

The Feynman rules for the Lagrangian Eq. (1) are given in Appendix B.

A. Tree amplitude

The tree amplitude for $w^+ w^- \rightarrow zz$ is found from the diagrams in Fig. 1 to be

$$\mathcal{A}_{\text{tree}} = \frac{s}{v^2} - \left(\frac{\xi^2}{v^2}\right) \frac{s^2}{s - m^2}, \quad (37)$$

where s, t, u are the usual Mandelstam variables with $s + t + u = 0$. For $\sqrt{s} \ll m, v$ only the first term (coming solely from the Goldstone boson contact diagram) survives; this corresponds to the low-energy theorems [9,25]. For somewhat higher energies, deviations from the SM emerge and these are parametrized by just one parame-

⁴The relatively light a in Eq. (33) does not survive when other symmetry breaking terms are included or for larger values of f . Furthermore, the a does not appear as an s -channel pole in WW scattering and the fact that it is relatively light would not affect the discussion in the next section.

⁵An interesting alternative that includes potentially light scalars is technicolor models with additional fundamental scalars [24]. However, in contrast to the $SU(4)/Sp(4)$ model presented above, these do not reduce to the standard model by taking any particular limit.

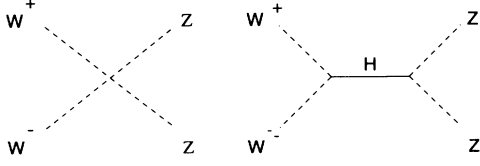


FIG. 1. The tree-level Feynman diagrams contributing to $w^+ w^- \rightarrow zz$.

ter ξ . For $\xi \neq 1$, the tree amplitude in Eq. (37) has a bad high-energy behavior, as expected for a nonrenormalizable effective theory. In fact, for $\xi < 1$ the amplitude vanishes for some energy greater than m^2 . However, in this region, the tree amplitude is not trustworthy since higher order effects will be large. Furthermore, in the region around the peak $s = m^2$ we have to include the Higgs decay width. This is done through the substitution

$$\frac{i}{s - m^2} \rightarrow \frac{i}{s - m^2 - i\text{Im}\Pi_H^{(1)}(s)}, \quad (38)$$

where $\Pi_H^{(1)}(s)$ is the one-loop self-energy given in Eq. (41) below.⁶

B. One-loop amplitude

We now present the one-loop amplitudes which are formally of order $O(p^4)$ in the chiral expansion. These are calculated using $\overline{\text{MS}}$ regularization with the infinities in the diagrams (which correspond to poles in $1/\epsilon$) omitted. Hence the parameters $m, v, \xi, \xi', \xi'', \lambda_3, \lambda_4$ that appear in the expressions below are actually the $\overline{\text{MS}}$ renormalized quantities. The corresponding physical Higgs mass and (VEV), denoted here as m_H, ν , are obtained from m, v by a finite renormalization⁷

$$\nu^2 = Z_v^{-1} v^2, \quad (39)$$

$$m_H^2 = m^2 + \delta m^2,$$

with $\nu=246$ GeV and

$$\delta m^2 = \text{Re}\Pi_H^{(1)}(m_H^2) \quad (40)$$

with $\Pi_H^{(1)}(p^2)$ the one-loop Higgs self-energy given by Eq. (41) below, with $G(1) = -2 + \pi/\sqrt{3}$. We used above that $Z_v = Z_w$, the wave-function renormalization of the w^a . This is found either directly, by minimizing the one-loop effective potential and determining the shift from v , or by using the Ward identity that ensures the equivalence theorem.⁸ Let us remark finally that the slightly uncon-

⁶The inclusion of the running width instead of the constant one has been suggested [32] to be more effective on peak.

⁷Actually m_H is the on-shell mass and not the real part of the pole position.

⁸See Eq. (4.11)–(4.13) in the paper by Bagger and Schmidt in Ref. [10] and also [33].

ventional choice of the VEV v as a running quantity is substituted in the more traditional treatments of electroweak radiative corrections by the mass of the gauge boson M_W , since $M_W = gv/2$. For our purpose the differences between various definitions of g are negligible [34].

1. Self-energy contributions

The Higgs self-energy $\Pi_H^{(1)}(p^2)$ is found from the diagrams of Fig. 2(a) to be

$$\Pi_H^{(1)}(s) = -\frac{1}{16\pi^2} \left\{ \frac{3\xi^2 s^2}{2v^2} B_1(s) + \frac{m^2 \lambda_4}{2} A(m) - \frac{\lambda_3^2 v^2}{2} \left[1 + G\left(\frac{s}{m^2}\right) \right] \right\}. \quad (41)$$

Analytical expressions for the functions used are given in Appendix C. The imaginary part of the one-loop self-energy $\Pi_H^{(1)}$ is related to the decay width through a unitarity cut

$$\text{Im}\Pi_H^{(1)}(m^2) = -m\Gamma_H^{(0)} \quad (42)$$

and is given by

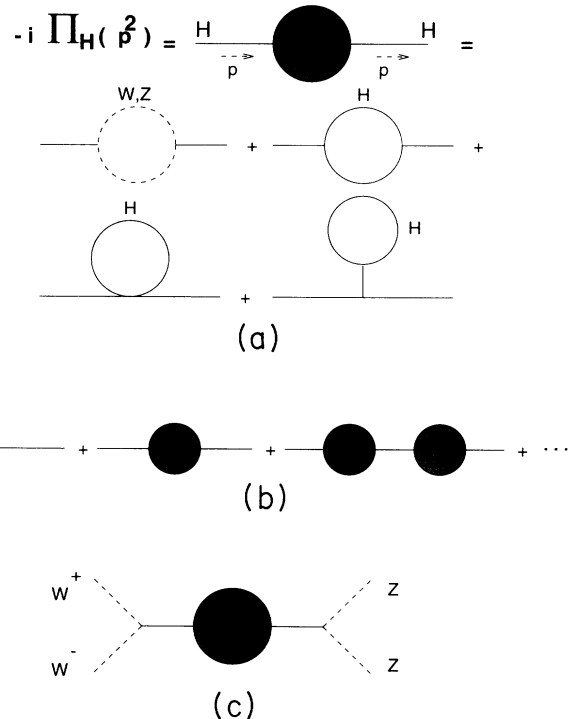


FIG. 2. (a) One-loop Higgs boson self-energy. (b) Sum of diagrams that replaces the propagator on the resonance region. (c) Higgs boson self-energy contribution to $w^+ w^- \rightarrow zz$. As explained in Sec. III B 1, for energies around the Higgs mass the resummed propagator is used from diagrams of Fig. 2(b).

$$\Gamma_H^{(0)} = \frac{3m^3}{32\pi v^2} \xi^2. \quad (43)$$

Since the parameter ξ can only be $\xi < 1$ in the $SU(4)/Sp(4)$ model, we see that in this model such a Higgs would be narrower than the SM Higgs boson.⁹

The one-loop contribution of $\Pi_H^{(1)}(s)$ to $w^+w^- \rightarrow zz$, for energies away from the Higgs-boson pole, is given by

$$\mathcal{A}_{2-pt} = - \left(\frac{\xi^2}{v^2} \right) \frac{s^2 \Pi_H^{(1)}(s)}{(s - m^2)^2}. \quad (44)$$

In the resonance region, $|s - m^2| \leq m\Gamma_H$, again we have to include the Higgs decay in the propagator. However, now, if we want to count powers of $\lambda' (\equiv m^2/2v^2)$ (which in the linear σ model is the self-coupling λ) consistently on the peak, we have to resum not only the imaginary part of the one-loop Higgs self-energy but also its real part along with the imaginary part of the two-loop Higgs self energy $\Pi_H^{(2)}(s)$. Furthermore, since we are using a nonlinear representation of the Goldstone bosons, the inclusion of the width is consistent with the equivalence theorem [35]. Hence, the Higgs self-energy contribution on peak to $w^+w^- \rightarrow zz$, is found by making the replacement (in order to avoid double counting) of the second diagram in Fig. 1, which corresponds to the second term in Eq. (37), with the diagram in Fig. 2(c) with the propagator given by

$$\frac{i}{s - m^2} \rightarrow \frac{i}{s - m^2 - \Pi_H^{(1)}(s) - i\text{Im}\Pi_H^{(2)}(s)}. \quad (45)$$

With this resummation procedure our complete amplitude is correct to order $O(\lambda')$ on the peak (see [37]). The imaginary part of $\Pi_H^{(2)}(s)$ at $s = m^2$ can be found from the one-loop correction, $\Gamma_H^{(1)}$, to the Higgs decay width through a unitarity cut similar to that of Eq. (42) at the appropriate order. This is presented in the following section.

From Π_H in Eq. (41), and the Goldstone boson self-energy Π_w , given by the diagrams in Fig. 3, we find the wave-function renormalization factors, defined as

$$-i \Pi_W(p^2) = \begin{array}{c} \text{W} \text{---} \text{H} \text{---} \text{W} \\ \text{p} \rightarrow \end{array} + \begin{array}{c} \text{H} \\ \text{W} \text{---} \text{W} \\ \text{p} \rightarrow \end{array} + \begin{array}{c} \text{H} \\ \text{W} \text{---} \text{W} \\ \text{p} \rightarrow \end{array}$$

FIG. 3. The one-loop gauge boson self-energy.

⁹In models with elementary scalars, since no scalar VEV can exceed 246 GeV, ξ must be less than one. The possibility that $\xi > 1$ was demonstrated recently in Ref. [36].

$$Z_w = 1 + \text{Re} \frac{d\Pi_w}{dp^2} \Big|_{p^2=0},$$

$$Z_H = 1 + \text{Re} \frac{d\Pi_H}{dp^2} \Big|_{p^2=m^2},$$

to be given by

$$Z_w^{1/2} = 1 - \frac{m^2}{32\pi^2 v^2} \left\{ \frac{\xi^2}{2} + \left[\xi^2 - \xi' + \frac{\xi \lambda_3 v^2}{m^2} \right] A(m) \right\}, \quad (46)$$

$$Z_H^{1/2} = 1 - \frac{1}{32\pi^2} \left\{ \frac{3\xi^2 m^2}{v^2} \left[\frac{1}{2} + A(m) \right] - \frac{\lambda_3^2 v^2}{2m^2} \left(1 - \frac{2\pi\sqrt{3}}{9} \right) \right\}. \quad (47)$$

2. Vertex corrections

The Hw^+w^- and Hzz three-point functions contribute to $w^+w^- \rightarrow zz$ scattering through the diagrams shown in Fig. 4. The Hw^+w^- three-point function is

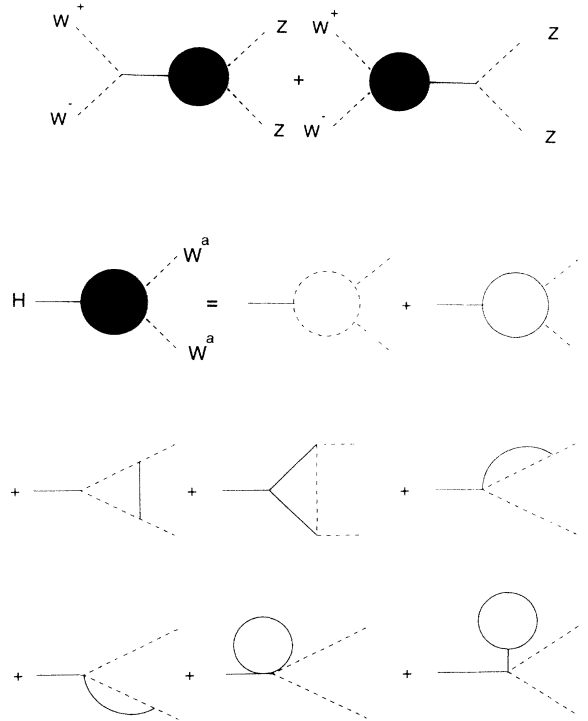


FIG. 4. The one-loop contribution to $w^+w^- \rightarrow zz$ scattering amplitude through the Hw^+w^- vertex.

$$\begin{aligned}
i\Gamma(s) = & \frac{i}{16\pi^2 v^3} \left\{ -\xi\xi' m^2 s - \xi s^2 B_1(s) - \frac{\xi' \lambda_3 v^2}{2} s \left[1 + G\left(\frac{s}{m^2}\right) \right] \right. \\
& - (\xi'' + \xi\xi') m^2 s A(m) + \xi^3 s \left[\frac{m^2}{2} + \left(m^2 - \frac{s}{2}\right) B_1(s) - m^2 C_1(s) \right] \\
& \left. + \xi^2 \lambda_3 v^2 \left[m^2 A(m) - \left(\frac{s}{2} + m^2\right) B_2(s) - m^2 C_2(s) \right] \right\}. \quad (48)
\end{aligned}$$

Isospin variance implies that the Hzz vertex is identical to the Hw^+w^- vertex. This contribution to the $w^+w^- \rightarrow zz$ amplitude is

$$\mathcal{A}_{3\text{-pt}} = \left(\frac{\xi}{v}\right) \frac{2s\Gamma(s)}{s - m^2}, \quad (49)$$

where the replacement in Eq. (45) is needed in the resonance region.

From the proper three-point function we can compute the decay width of the Higgs at one loop, by adding to the tree amplitude the real part of $\Gamma(s)$ (for $s = m^2$), and

multiplying each external H, w^a line by wave-function renormalization factors $Z_H^{1/2}, Z_w^{1/2}$, respectively. This gives

$$\left(-\frac{\xi m_H^2}{\nu} + \text{Re}\Gamma(m_H)\right) Z_w^{1/2} Z_H^{1/2}, \quad (50)$$

where we have used Eq. (39) to replace v with $\nu=246$ GeV in the tree amplitude. Then the one-loop correction $\Gamma_H^{(1)}$ to the total Higgs decay width $\Gamma_H^{1\text{-loop}} = \Gamma_H^{(0)} + \Gamma_H^{(1)}$, is found to be (this result differs from that presented in [14]; we have corrected a typographical error in the next-to-last term)

$$\begin{aligned}
\frac{\Gamma_H^{(1)}}{\Gamma_H^{(0)}} = & \frac{1}{8\pi^2} \left\{ \frac{m^2}{v^2} [1 + A(m)] + \frac{\xi' \lambda_3}{2\xi} \left(\frac{\pi}{\sqrt{3}} - 1\right) + \frac{\lambda_3^2 v^2}{4m^2} \left(1 - \frac{2\pi\sqrt{3}}{9}\right) + \frac{\xi'' m^2}{\xi v^2} A(m) \right. \\
& \left. + \xi' \frac{3m^2}{2v^2} \left(\frac{1}{3} + A(m)\right) + \frac{\xi^2 m^2}{2v^2} \left(\frac{\pi^2}{6} - 4 - 5A(m)\right) - \frac{\xi \lambda_3}{2} \left[\pi\sqrt{3} - 3 - \frac{2\pi^2}{9}\right] \right\}, \quad (51)
\end{aligned}$$

where we used the explicit form of the B, C functions presented in Appendix C. In the linear σ -model limit, Eqs. (4),(5), our calculations agree with those in Refs. [34,31]. For our reference values of Eq. (36), the one-loop correction to the three-level width in Eq. (43) is 28%, while the corresponding standard model correction is only 7.6%.

3. One-particle-irreducible corrections

The one-particle-irreducible (1PI) diagrams that contribute are shown in Fig. 5. The bubble diagrams in Fig. 5(a) give the chiral logarithmic corrections from the nonlinear sigma model. They are given by

$$\mathcal{A}_{\text{GB}} = \frac{1}{(4\pi v^2)^2} \left(\frac{5}{9} s^2 + \frac{13}{18} (t^2 + u^2) + \frac{s^2}{2} \ln \frac{\mu^2}{-s} + \frac{t}{6} (s + 2t) \ln \frac{\mu^2}{-t} + \frac{u}{6} (s + 2u) \ln \frac{\mu^2}{-u} \right). \quad (52)$$

The rest of the diagrams with two internal propagator given in Fig. 5(b) are

$$\mathcal{A}_{\text{bubble}} = \frac{1}{(4\pi v^2)^2} \left[\frac{\xi'^2}{2} s^2 B_2(s) + 2\xi^2 m^2 s \left(\frac{1}{2} + A(m)\right) \right]. \quad (53)$$

The diagrams with three internal propagators shown in Fig. 5(c) are given by

$$\begin{aligned}
\mathcal{A}_{1\text{-tri}} = & \frac{2\xi^2}{3(4\pi v^2)^2} \left[\frac{2s^2 - t^2 - u^2}{6} - 3m^2 s + 6m^2 \left(m^2 + \frac{s}{2} - \frac{m^2 s^2}{tu}\right) A(m) \right. \\
& + 3s \left(\frac{s}{2} - m^2\right) B_1(s) - \left(3m^4 + t^2 + \frac{st}{2} - \frac{3}{2} m^2 t + 6m^4 \frac{s}{t}\right) B_1(t) \\
& - \left(3m^4 + u^2 + \frac{su}{2} - \frac{3}{2} m^2 u + 6m^4 \frac{s}{u}\right) B_1(u) + 3m^2 s C_1(s) \\
& \left. + 3m^2 \left(s + m^2 + 2m^2 \frac{s}{t}\right) C_1(t) + 3m^2 \left(s + m^2 + 2m^2 \frac{s}{u}\right) C_1(u) \right] \quad (54)
\end{aligned}$$

while the rest with three internal propagators in Fig. 5(d) are

$$\mathcal{A}_{2\text{-tri}} = \frac{2\xi^2\xi'}{(4\pi v^2)^2} \left[m^2 s A(m) - \left(\frac{s^2}{2} + m^2 s \right) B_2(s) - m^2 s C_2(s) \right]. \quad (55)$$

The diagrams in Fig. 5(e), with four internal propagators are equal to

$$\mathcal{A}_{\text{box}} = \mathcal{I}(s, t) + \mathcal{I}(s, u), \quad (56)$$

where

$$\begin{aligned} \mathcal{I}(s, t) = & \frac{\xi^4}{(4\pi v^2)^2} \left\{ \frac{s^2 + t^2 + 4st}{18} + \frac{m^2}{3} (2s + t) \right. \\ & - m^2 \left[6m^2 + \frac{1}{3}(2s - 5t) + 4m^2 \left(\frac{s}{t} + \frac{t}{s} \right) \right] A(m) \\ & + \left(3m^4 + 4m^4 \frac{s}{t} - m^2 t + \frac{t}{6}(s + 2t) \right) B_1(t) \\ & + \left(3m^4 + \frac{2}{3}m^2(s - t) + 4m^4 \frac{t}{s} + \frac{s}{6}(2s + t) \right) B_2(s) \\ & + 2m^2 \left(2m^2 - t + 2m^2 \frac{t}{s} \right) C_2(s) - 2m^2 \left(2m^2 + s + 2m^2 \frac{s}{t} \right) C_1(t) \\ & \left. + m^4 D(s, t) \right\}. \quad (57) \end{aligned}$$

4. Tadpoles

The contribution from the tadpole diagrams shown in Fig. 6 is

$$\mathcal{A}_{\text{tad}} = \frac{1}{(4\pi v^2)^2} \{ \xi \lambda_3 v^2 - \xi' m^2 \} s A(m). \quad (58)$$

5. Complete one-loop amplitude

Adding all the one-loop contributions from above, and multiplying by a factor of $Z_w^{1/2}$ for each external line we find that the complete one-loop correction to the $w^+ w^- \rightarrow zz$ amplitude is given by

$$\begin{aligned} \mathcal{A}_{1\text{-loop}} = & \mathcal{A}_{2\text{-pt}} + \mathcal{A}_{3\text{-pt}} + \mathcal{A}_{\text{GB}} + \mathcal{A}_{\text{bubble}} + \mathcal{A}_{1\text{-tri}} \\ & + \mathcal{A}_{2\text{-tri}} + \mathcal{A}_{\text{box}} + \mathcal{A}_{\text{tad}} + 4\mathcal{A}_{\text{tree}}(Z_w^{1/2} - 1). \quad (59) \end{aligned}$$

As explained, our results here are expressed in terms of the renormalized mass and VEV. The physical parameters are found through the relations (39). We have verified explicitly that, in the linear σ -model limit, Eqs.

(4),(5), our computation is scale independent and reproduces the calculation of Ref. [31]. This provides a non-trivial check of our calculation.

For the sake of completeness we present here the low-energy limit of our amplitude which constitutes the p^4 corrections to the low-energy theorems [14]. For this we use the low-energy limit of the functions provided in Appendix C. These can be found, for example, in Appendix A of Ref. [38]. Let us call the total amplitude for $w^+ w^- \rightarrow zz$, up to one loop, by

$$\mathcal{A}(s, t, u) = \mathcal{A}_{\text{tree}} + \mathcal{A}_{1\text{-loop}}. \quad (60)$$

In the limit $s \ll m^2$ and $-t \ll m^2$, we find

$$\mathcal{A}(s, t, u) = \frac{s}{v^2} + \frac{1}{(4\pi v^2)^2} \mathcal{T} + \xi^2 \frac{s^2}{m^2 v^2}, \quad (61)$$

$$\begin{aligned} \mathcal{T} = & \frac{s^2}{2} \ln \frac{\mu^2}{-s} + \frac{t}{6} (s + 2t) \ln \frac{\mu^2}{-t} + \frac{u}{6} (s + 2u) \ln \frac{\mu^2}{-u} \\ & + s^2 P + Q(t^2 + u^2) + R \ln \frac{m^2}{\mu^2}, \quad (62) \end{aligned}$$

where

$$P = \frac{5}{9} + 2\xi\xi'' + \xi^2 \left(\frac{7}{2}\xi' + \frac{22}{9} \right) - \frac{65}{9}\xi^4 + \frac{\xi\lambda_3}{2\lambda'} \left(\xi' - \frac{\xi^2}{2} \right) + \xi^2 \frac{\lambda_3^2}{8\lambda'^2} \left(\frac{\pi}{\sqrt{3}} - 2 \right), \quad (63)$$

$$Q = \frac{13}{18} - \frac{11}{9}\xi^2 + \frac{5}{18}\xi^4, \quad (64)$$

$$R = s^2 \left[\frac{37}{6}\xi^4 - \xi^2 \left(\frac{10}{3} + 2\xi' \right) + 2\xi\xi'' - \frac{\xi'^2}{2} \right] + \frac{\xi^2}{3} (2 - \xi^2)(t^2 + u^2), \quad (65)$$

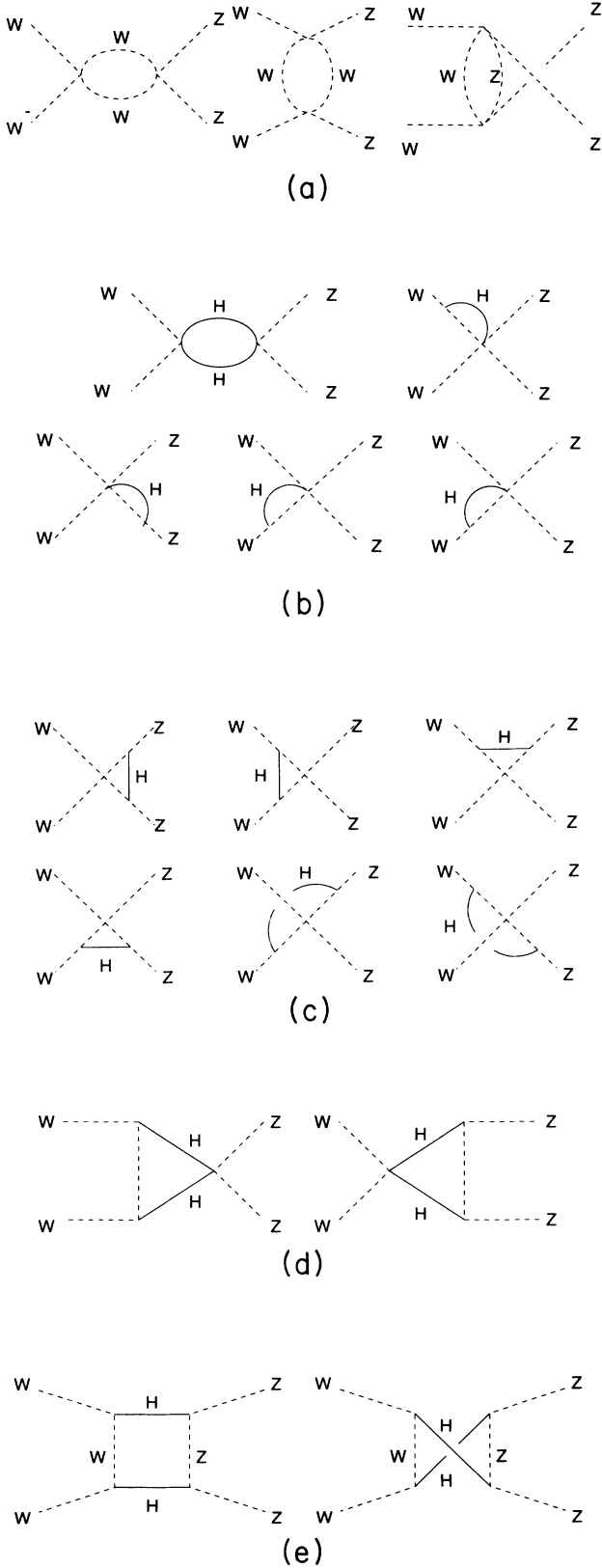


FIG. 5. (a) Bubble diagrams that contribute to $w^+w^- \rightarrow zz$. (b) The rest of the 1PI diagrams with two internal propagators. (c), (d) Feynman diagrams with three internal propagators. (e) Feynman diagrams with four internal propagators.

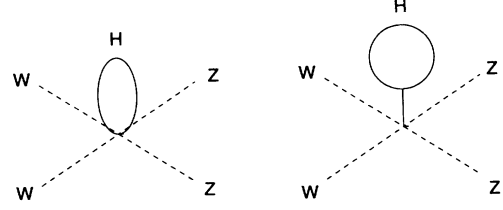


FIG. 6. The tadpole diagrams.

where $\lambda' = m^2/2v^2$. Also in Eq. (61), and since $m < 4\pi v$, we have retained the $1/m^2$ correction to this order in the momentum expansion. In the linear σ -model limit and to leading order in s/m^2 this amplitude explicitly agrees with that of Ref. [31].

The scattering amplitudes for all other channels can be obtained from the $w^+w^- \rightarrow zz$ amplitude $\mathcal{A}(s, t, u)$. In terms of the kinematical variables s, t, u , these are given by

$$\mathcal{A}(w^+w^- \rightarrow zz) = \mathcal{A}(s, t, u) ,$$

$$\mathcal{A}(w^+w^- \rightarrow w^+w^-) = \mathcal{A}(s, t, u) + \mathcal{A}(t, s, u) ,$$

$$\mathcal{A}(z \rightarrow zz) = \mathcal{A}(s, t, u) + \mathcal{A}(t, s, u) + \mathcal{A}(u, t, s) , \quad (66)$$

$$\mathcal{A}(w^+w^+ \rightarrow w^\pm w^\pm) = \mathcal{A}(t, s, u) + \mathcal{A}(u, t, s) ,$$

$$\mathcal{A}(w^\pm z \rightarrow w^\pm z) = \mathcal{A}(t, s, u) .$$

C. Cross section and discussion

The differential cross section for longitudinal gauge boson scattering in any of these channels is obtained from the amplitudes above by

$$\frac{d\sigma}{dt} = \frac{1}{16\pi s^2} |\mathcal{A}|^2 , \quad (67)$$

where $\mathcal{A} = \mathcal{A}_{\text{tree}} + \mathcal{A}_{\text{loop}}$. Since we neglected the 1-PI two-loop diagrams, we have

$$|\mathcal{A}|^2 = |\mathcal{A}_{\text{tree}}|^2 + 2[\text{Re}(\mathcal{A}_{\text{tree}})\text{Re}(\mathcal{A}_{\text{loop}}) + \text{Im}(\mathcal{A}_{\text{tree}})\text{Im}(\mathcal{A}_{\text{loop}})] . \quad (68)$$

The total cross section is

$$\sigma_{\text{tot}}(s) = \int_{-s}^0 dt \frac{d\sigma}{dt}(s, t) . \quad (69)$$

In Fig. 7(a) we show the total cross section for the $W_L^+W_L^- \rightarrow W_L^+W_L^-$ channel as a function of s , for the SU(4)/Sp(4) model with the parameters in Eq. (36). As was explained in Sec. III B 1, our one-loop amplitude is

accurate in the resonance region only up to order λ' . Our calculation respects unitarity to the appropriate order in perturbation theory, however, the computation also includes some (*but not all*) subleading contributions. These contributions can be numerically significant on the peak and appear to cause a violation of unitarity [37]. The height of the peak for the one-loop curve is 4.5% higher than the peak in the tree-level curve. The corresponding curves for a standard model Higgs boson with the same mass are shown in Fig. 7(b); here the one-loop peak exceeds the tree-level peak by 11%. The sharp fall in the amplitude in the region above the peak can be understood by noting that for $\xi < 1$ the tree amplitude in Eq. (37) vanishes at some energy greater than m^2 (if one does not include a finite width). This only signals that higher order effects are expected to be significant there. Also, far above the peak the amplitude presented is not trustworthy due to the breakdown of the expansion in powers of $1/\Lambda$.

Qualitatively, however, for gauge boson scattering be-

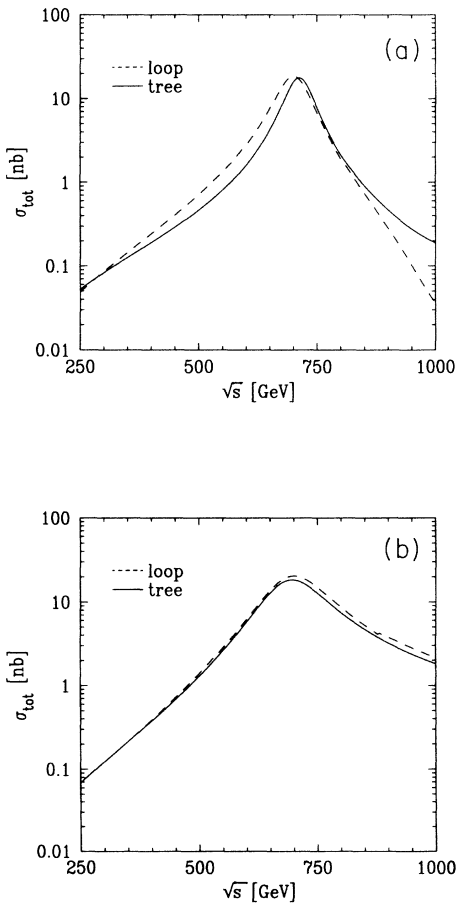


FIG. 7. (a) Total cross section for $W_L^+ W_L^- \rightarrow W_L^+ W_L^-$, in the SU(4)/Sp(4) with a Higgs mass $m_H=718$ GeV, and using the values in Eq. (36) as a function of s . Solid lines correspond to tree level and dashed lines to one loop. (b) Total cross section for $W_L^+ W_L^- \rightarrow W_L^+ W_L^-$ in the standard model with a Higgs mass $m_H=718$ GeV, as a function of s . Solid lines correspond to tree level and dashed lines to one-loop.

low a TeV, the width and shape of the peak appear to be the most important features differentiating a standard from a nonstandard Higgs boson resonance. In Fig. 8(a) we show the decay width Γ_H as a function of mass for the nonlinear model for our reference values in Eq. (36), both at tree level and one loop, while the corresponding graph for the standard model is shown in Fig. 8(b).

The cross sections discussed above are not directly measurable in hadron colliders like the LHC; one must first convolute them with the $W_L W_L$ luminosities inside the proton. A more detailed study of how well the LHC would be able to differentiate a standard from a nonstandard Higgs can only be answered after detailed analysis of a specific detector. This question is currently under investigation [40]. Unlike the analysis presented here, however, one must also include the potentially nonstandard couplings of this nonstandard Higgs to the top quark, since this affects the production of the Higgs through gluon fusion.

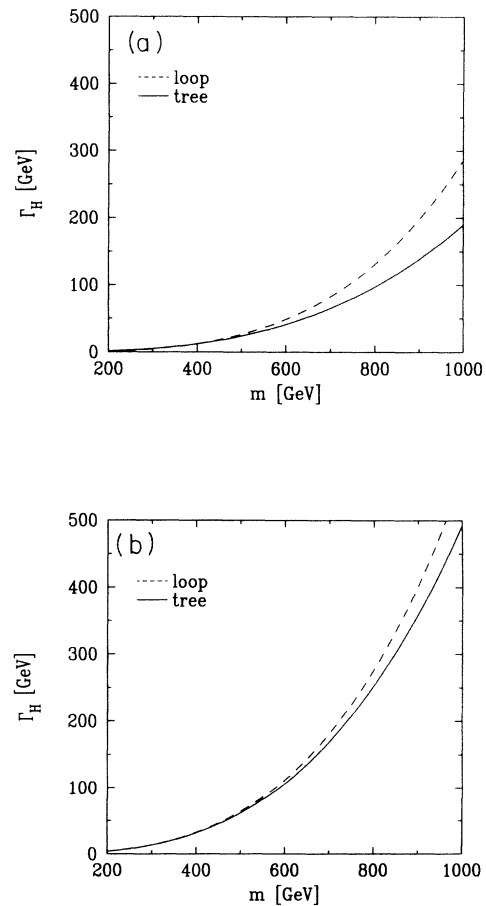


FIG. 8. (a) Total Higgs decay width as a function of the Higgs mass for the SU(4)/Sp(4) model with the choice in Eq. (36). Solid lines correspond to tree level and dashed lines to one loop. (b) Total Higgs decay width as a function of the Higgs mass for the standard model. Solid lines correspond to tree level and dashed lines to one loop.

IV. CONCLUSIONS

In this paper, we consider the phenomenology of a “nonstandard” Higgs boson. In the first half of our analysis, we discussed a composite Higgs model based on an $SU(4)/Sp(4)$ nonlinear σ model that features such a nonstandard Higgs boson. This model illustrates the possibility of the existence of a scalar resonance that is relatively light (possibly within the reach of the LHC), but whose dynamics is significantly different from that of the standard model Higgs Boson. Unlike conventional technicolor models, composite Higgs models may have a large mass gap between the Higgs resonance and the other heavier resonances and, therefore, one cannot necessarily rely on the discovery of the other, more exotic, resonances as an experimental signature of the dynamics. Instead, it will be important to understand whether the light scalar resonance has the properties of a standard model Higgs resonance or not.

Furthermore, because of the triviality of fundamental scalar theories, *any* scalar boson with a mass of order 500 GeV or higher that couples to the longitudinal electroweak gauge bosons is likely to have properties very different than those of the standard model Higgs boson.

In the second half of our analysis we calculated the chiral logarithmic corrections to longitudinal gauge boson scattering in a theory with a nonstandard Higgs resonance. We found that the most important deviations from the standard model are parametrized by the parameter ξ , which is directly related to the Higgs width.

The understanding of the electroweak symmetry sector will surely require further experimental investigation.

If a scalar isoscalar resonance is observed in longitudinal gauge boson scattering, it will be important to show whether or not it is the standard model Higgs boson.

ACKNOWLEDGMENTS

We would like to thank Mitchell Golden, Dimitris Kominis, Stephen Selipsky, and Elizabeth Simmons for helpful discussions and suggestions. V.K. also thanks Ulrich Nierste for checking the form of the box diagram given in Appendix C. R.S.C. acknowledges the support of the Alfred P. Sloan Foundation, the NSF, the DOE, and the Texas National Research Laboratory Commission. This work was supported in part under NSF contract PHY-9057173 and DOE Contract No. DE-FG02-91ER40676, and by funds from the Texas National Research Laboratory Commission under Grant No. RGFY92B6.

APPENDIX A

In this appendix we give the expression for the Lagrangian of the $SU(4)/Sp(4)$ that we mentioned in Sec. II. Making the field redefinition given by Eqs. (24)–(26), we have

$$\Sigma_0 = \cos\left(\frac{\sigma + \langle\sigma\rangle}{\sqrt{2}f}\right) + i2\sqrt{2}X \sin\left(\frac{\sigma + \langle\sigma\rangle}{\sqrt{2}f}\right) \quad (\text{A1})$$

and the $SU(4)/Sp(4)$ Lagrangian Eq. (19) is

$$\begin{aligned} \mathcal{L}_f = & \frac{1}{2}(\partial^\mu\sigma\partial_\mu\sigma) + \frac{f^2}{2}\sin^2\left(\frac{\sigma + \langle\sigma\rangle}{\sqrt{2}f}\right) \text{Tr}(\partial^\mu\mathcal{U}\partial_\mu\mathcal{U}^\dagger) - V(\sigma, \sigma') + \frac{1}{2}\partial^\mu\sigma'\partial_\mu\sigma' \\ & + \frac{1}{4}\left(\frac{\sigma' + \langle\sigma'\rangle}{\sqrt{2}f}\right)^2 \text{Tr}(\partial^\mu\mathcal{V}\partial_\mu\mathcal{V}^\dagger) \\ & - \frac{\sqrt{2}fm_p^2}{v^2\sin 2\alpha}(\sigma' + \langle\sigma'\rangle)\sin\left(\frac{\sigma + \langle\sigma\rangle}{\sqrt{2}f}\right) \mathbf{p} \cdot \mathbf{p} , \end{aligned} \quad (\text{A2})$$

where $V(\sigma, \sigma')$ is the potential in Eq. (20), expressed in terms of the shifted fields σ, σ' . Above we have ignored the singlet field a , and terms with more pseudoscalars \mathbf{p} , coming from \mathcal{L}_{Yuk} , since these will not be relevant to our calculation. The \mathbf{p} and a masses are

$$m_p^2 = \frac{2y\mu f}{\sin 2\alpha}, \quad m_a^2 = y\mu f \tan\alpha . \quad (\text{A3})$$

In the Lagrangian above, there are some individual diagrams, like the $H p^a p^a$ vertex coming from the \mathcal{L}_{Yuk} , that grow like f^2/v . Such terms would appear to violate the decoupling of the \mathbf{p} as $f \rightarrow \infty$. However before the redef-

inition of Eq. (25), there are no terms that grow with f . The resolution to this dilemma lies in a general theorem in quantum field theory [11,21], according to which all physical on-shell S -matrix elements are invariant under field redefinitions that leave unchanged the one-particle states, which constitute the Hilbert space of the theory. Indeed, one can easily verify that, when evaluating any S -matrix element, the bad large- f behavior cancels when the external lines go on shell.

Finally, after “integrating out” the heavy states \mathbf{p} , h , and a , we obtain the Lagrangian in Eq. (1). The parameters $\xi, \xi', \xi'', \lambda_3, \lambda_4$ are given by

$$\xi = \sin\alpha \sin\beta + \cos\alpha \cos\beta \sqrt{1 - \frac{v^2 \cos^2 \alpha}{2f^2}},$$

$$\xi' = 1 - \frac{v^2}{f^2} \cos^2 \alpha \cos^2 \beta,$$

$$\xi'' = \frac{v^2}{f^2} \cos\alpha \cos^3 \beta \sqrt{1 - \frac{v^2 \cos^2 \alpha}{2f^2}},$$

$$\lambda_3 = 6v(\lambda \sin\alpha \sin^3 \beta + \pi y \cos\alpha \sin\beta \cos^2 \beta),$$

$$\lambda_4 = 6\lambda \sin^4 \beta + 2\pi y \cos^3 \beta$$

$$\times \left(4\sin\beta \sqrt{1 - \frac{v^2 \cos^2 \alpha}{2f^2}} - \tan\alpha \cos\beta \right). \quad (\text{A4})$$

APPENDIX B

In this appendix we give the Feynman rules for the Lagrangian in Eq. (1).

$$H \text{ --- } \overset{p \longrightarrow}{\text{---}} \text{ --- } H$$

$$\frac{i}{p^2 - m^2}$$

$$w^a \text{ --- } \overset{p \longrightarrow}{\text{---}} \text{ --- } w^a$$

$$\frac{i}{p^2}$$

$$H \text{ --- } \begin{array}{l} \nearrow^{p_1} \text{---} w^{+,z} \\ \searrow_{p_2} \text{---} w^{-,z} \end{array}$$

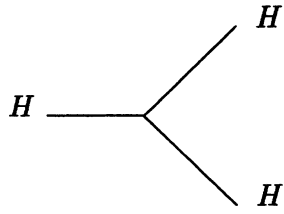
$$-i\xi \frac{2p_1 \cdot p_2}{v}$$

$$\begin{array}{l} H \text{ ---} \\ H \text{ ---} \end{array} \begin{array}{l} \nearrow^{p_1} \text{---} w^{+,z} \\ \searrow_{p_2} \text{---} w^{-,z} \end{array}$$

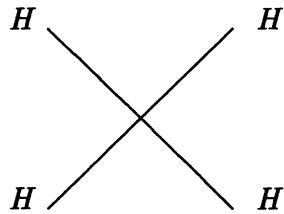
$$-i\xi' \frac{2p_1 \cdot p_2}{v^2}$$

$$\begin{array}{l} H \text{ ---} \\ H \text{ ---} \\ H \text{ ---} \end{array} \begin{array}{l} \nearrow^{p_1} \text{---} w^{+,z} \\ \searrow_{p_2} \text{---} w^{-,z} \end{array}$$

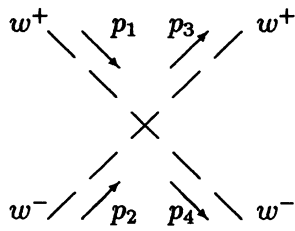
$$i\xi'' \frac{4p_1 \cdot p_2}{v^3}$$



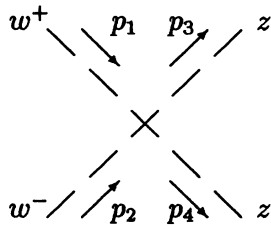
$$-i\lambda_3 v$$



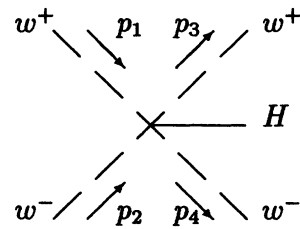
$$-i\lambda_4$$



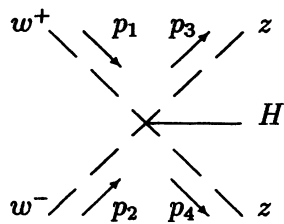
$$\frac{i}{3v^2} [2p_1 \cdot p_4 + 2p_2 \cdot p_3 + (p_1 - p_4) \cdot (p_2 - p_3)]$$



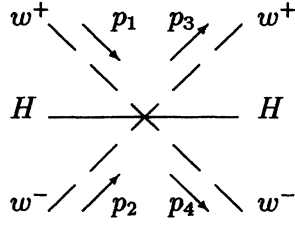
$$\frac{i}{3v^2} [2p_1 \cdot p_2 + 2p_3 \cdot p_4 + (p_1 + p_2) \cdot (p_3 + p_4)]$$



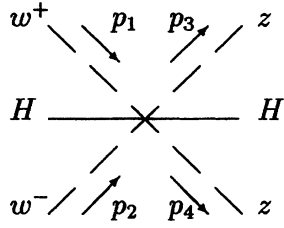
$$\frac{2i\xi}{3v^3} [2p_1 \cdot p_4 + 2p_2 \cdot p_3 + (p_1 - p_4) \cdot (p_2 - p_3)]$$



$$\frac{2i\xi}{3v^3} [2p_1 \cdot p_2 + 2p_3 \cdot p_4 + (p_1 + p_2) \cdot (p_3 + p_4)]$$



$$\frac{2i\xi'}{3v^4} [2p_1 \cdot p_4 + 2p_2 \cdot p_3 + (p_1 - p_4) \cdot (p_2 - p_3)]$$



$$\frac{2i\xi'}{3v^4} [2p_1 \cdot p_2 + 2p_3 \cdot p_4 + (p_1 + p_2) \cdot (p_3 + p_4)]$$

APPENDIX C

In this appendix we provide the analytic expressions for the one-loop integrals that appear in the text. Here, μ is the renormalization scale. In our computation we shall take μ to be the cutoff of our effective theory $\Lambda \simeq 4\pi f$. We use the notation

$$\sigma = s/m^2, \quad \tau = t/m^2, \quad (\text{C1})$$

and define the dilogarithm for arbitrary complex argument by

$$\text{Li}_2(x) = -\int_0^1 dt \frac{\ln(1-xt)}{t}. \quad (\text{C2})$$

Then we have

$$A(m) = 1 - \ln \frac{m^2}{\mu^2}, \quad (\text{C3})$$

$$B_1(s) = 2 - \ln \left(\frac{-s - i\epsilon}{\mu^2} \right), \quad (\text{C4})$$

$$B_2(s) = -\ln \frac{m^2}{\mu^2} - G(\sigma), \quad (\text{C5})$$

where

$$G(x) = \begin{cases} 2\sqrt{\frac{4-x}{x}} \arcsin \frac{\sqrt{x}}{2} - 2, & 0 < x \leq 4 \\ 2\sqrt{\frac{x-4}{x}} \left(-i\frac{\pi}{2} + \text{arccosh} \frac{\sqrt{x}}{2} \right) - 2, & x > 4 \\ 2\sqrt{\frac{x-4}{x}} \text{arcsinh} \frac{\sqrt{-x}}{2} - 2, & x \leq 0. \end{cases} \quad (\text{C6})$$

The functions $C_1(s), C_2(s)$ arise from loop diagrams with three internal propagators. Following Ref. [39] they are given by

$$C_1(s) = \frac{1}{\sigma} \left(\text{Li}_2(1 + i\epsilon + \sigma) - \frac{\pi^2}{6} \right), \quad (\text{C7})$$

$$C_2(s) = \frac{1}{\sigma} \left[\frac{\pi^2}{6} - \text{Li}_2 \left(\frac{1-\sigma}{1-i\epsilon\sigma} \right) - \text{Li}_2 \left(\frac{1}{1-\sigma l_+ - i\epsilon} \right) + \text{Li}_2 \left(\frac{1-\sigma}{1-\sigma l_+ - i\epsilon} \right) - \text{Li}_2 \left(\frac{1}{1-\sigma l_- + i\epsilon} \right) + \text{Li}_2 \left(\frac{1-\sigma}{1-\sigma l_- + i\epsilon} \right) \right]. \quad (\text{C8})$$

where

$$l_{\pm} = \frac{1}{2}(1 \pm \sqrt{1-4/\sigma}). \quad (\text{C9})$$

Finally the expression for the box diagram $D(s, t)$, following Ref. [41], is given by

$$\begin{aligned}
 (1 + \tau) \left(y - \frac{1}{y} \right) D(s, t) = & 2\text{Li}_2 \left(1 + \frac{z}{y} \right) - 2\text{Li}_2(1 + zy) + 4\text{Li}_2(1 + y) + \ln^2(-y) - \frac{1}{2}\ln^2(-zy) \\
 & + 2\ln(-y)\ln(-\tau - i\epsilon) - \eta(z, -y)\ln \left(2 + zy + \frac{1}{zy} \right) \\
 & - \eta \left(\frac{1}{z}, -y \right) \ln \left(2 + \frac{z}{y} + \frac{y}{z} \right)
 \end{aligned} \tag{C10}$$

with

$$\begin{aligned}
 z = 1 - \frac{\sigma}{2} + \left[\frac{\sigma^2}{4} - \sigma - i\epsilon \left(2 - \frac{\sigma}{2} \right) \right]^{1/2}, \\
 y = \frac{\sigma\tau - 2\tau - 2 + \sqrt{\sigma\tau(\sigma\tau - 4\tau - 4) + i\epsilon\tau(1 + \tau)}}{2(1 + \tau)},
 \end{aligned}$$

where

$$\eta(a, b) = \ln(ab) - \ln a - \ln b, \tag{C11}$$

as defined by 't Hooft, and Veltman [39].

-
- [1] D. Dicus and V. Mathur, *Phys. Rev. D* **7**, 3111 (1973).
[2] B. W. Lee, C. Quigg, and H. Thacker, *Phys. Rev. D* **16**, 1519 (1977).
[3] G. 't Hooft, in *Recent Developments in Gauge Theories*, edited by G. 't Hooft (Plenum, New York, 1980).
[4] K. G. Wilson, *Phys. Rev. B* **4**, 3184 (1971); K. G. Wilson and J. Kogut, *Phys. Rep.* **12**, 76 (1974); G. A. Baker and J. M. Kincaid, *J. Stat. Phys.* **24**, 469 (1981); M. Aizenmann, *Phys. Rev. Lett.* **47**, 1 (1981); *Commun. Math. Phys.* **86**, 1 (1982); J. Fröhlich, *Nucl. Phys.* **B200** [FS4], 281 (1982); A. D. Sokal, *Ann. Inst. H. Poincaré A* **37**, 317 (1982); C. Aragão de Carvalho, S. Caracciolo, and J. Fröhlich, *Nucl. Phys.* **B215**, 209 (1983); B. Freedmann, P. Smolensky, and D. Weingarten, *Phys. Lett.* **113B**, 481 (1982); for a review, see D. J. E. Callaway, *Phys. Rep.* **167**, 241 (1988).
[5] M. Lüscher and P. Weisz, *Nucl. Phys.* **B318**, 705 (1989); J. Kuti, L. Lin, and Y. Shen, *Phys. Rev. Lett.* **61**, 678 (1988); A. Hasenfratz, K. Jansen, C. B. Lang, T. Neuhaus, and H. Yoneyama, *Phys. Lett. B* **199**, 531 (1987); A. Hasenfratz, K. Jansen, J. Jersák, C. B. Lang, T. Neuhaus, and H. Yoneyama, *Nucl. Phys.* **B317**, 81 (1989); G. Bhanot, K. Bitar, U. M. Heller, and H. Neuberger, *ibid.* **B353**, 551 (1991).
[6] R. Dashen and H. Neuberger, *Phys. Rev. Lett.* **50**, 1897 (1983).
[7] See, for example, E. J. Eichten, C. Quigg, I. Hinchliffe, and K. D. Lane, *Rev. Mod. Phys.* **56**, 579 (1984).
[8] R. N. Cahn and S. Dawson, *Phys. Lett. B* **136**, 196 (1984).
[9] M. Chanowitz and M. K. Gaillard, *Nucl. Phys.* **B261**, 379 (1985).
[10] J. Cornwall, D. Levin, and G. Tiktopoulos, *Phys. Rev. D* **10**, 1145 (1974); C. Vayonakis, *Lett. Nuovo Cimento* **17**, 384 (1976); G. Gounaris, R. Kögerler, and H. Neufeld, *Phys. Rev. D* **34**, 3257 (1986); J. Bagger and C. Schmidt, *Phys. Rev. D* **41**, 264 (1990); H. Veltman, *Phys. Rev. D* **41**, 2 (1990); W. B. Kilgore, *Phys. Lett. B* **294**, 257 (1992); H. J. He and Y. P. Kuang, *Phys. Rev. Lett.* **69**, 2619 (1992).
[11] S. Coleman, J. Wess, and B. Zumino, *Phys. Rev.* **177**, 2239 (1969); C. G. Callan, S. Coleman, J. Wess, and B. Zumino, *Phys. Rev.* **177**, 2247 (1969).
[12] S. Weinberg, *Physica* **96A**, 327 (1979); H. Georgi and A. Manohar, *Nucl. Phys.* **B234**, 189 (1984); H. Georgi, *Phys. Lett. B* **298**, 187 (1993).
[13] For a review, see H. Georgi, *Weak Interactions and Modern Particle Theory* (Benjamin/Cummings, Menlo Park, CA, 1984).
[14] R. S. Chivukula and V. Koulovassilopoulos, *Phys. Lett. B* **309**, 371 (1993).
[15] D. B. Kaplan and H. Georgi, *Phys. Lett. B* **136**, 183 (1984).
[16] D. B. Kaplan, S. Dimopoulos, and H. Georgi, *Phys. Lett.* **136B**, 187 (1984); H. Georgi, D. B. Kaplan, and P. Galison, *ibid.* **143B**, 152 (1984); H. Georgi and D. B. Kaplan, *ibid.* **145B**, 216 (1984); M. J. Dugan, H. Georgi, and D. B. Kaplan, *Nucl. Phys.* **B254**, 299 (1985).
[17] E. Witten, *Phys. Lett.* **117B**, 324 (1982).
[18] M. E. Peskin, *Nucl. Phys.* **B175**, 197 (1980); J. Preskill, *ibid.* **B177**, 21 (1981).
[19] D. Kosower, *Phys. Lett.* **144B**, 215 (1984); C. Vafa and E. Witten, *Nucl. Phys.* **B234**, 1 (1984).
[20] H. Georgi, in *Architecture of Fundamental Interactions at Short Distances*, Proceedings of the Les Houches Summer School, Les Houches, France, 1985, edited by P. Ramond and R. Stora, Les Houches Summer School Proceedings Vol. 44 (Elsevier, New York, 1987), p. 339.
[21] S. Kamefuchi, L. O'Raiheartaigh, and A. Salam, *Nucl. Phys.* **28**, 529 (1961); R. Haag, *Phys. Rev.* **112**, 669 (1958); D. Ruelle, *Helv. Phys. Acta* **35**, 34 (1962); H. J. Borchers, *Nuovo Cimento* **25**, 270 (1960).

- [22] T. Appelquist and J. Carazzone, *Phys. Rev. D* **11**, 2856 (1975).
- [23] J. Gasser and H. Leutwyler, *Ann. Phys.* **158**, 142 (1984); *Nucl. Phys.* **B250**, 465 (1985).
- [24] E. H. Simmons, *Nucl. Phys.* **B312**, 253 (1989); S. Samuel, *ibid.* **B347**, 625 (1990); A. Kagan and S. Samuel, *Int. J. Mod. Phys. A* **7**, 1123 (1992); C. D. Carone and E. H. Simmons, *Nucl. Phys.* **B397**, 591 (1993); C. D. Carone and H. Georgi, *Phys. Rev. D* **49**, 1427 (1994).
- [25] M. S. Chanowitz, H. Georgi, and M. Golden, *Phys. Rev. D* **36**, 1490 (1987); *Phys. Rev. Lett.* **57**, 2344 (1986).
- [26] M. Golden, in *Beyond the Standard Model*, edited by K. Whisnant and B.-L. Young (World Scientific, Singapore, 1989), p. 111; A. Dobado and M. Herrero, *Phys. Lett. B* **228**, 495 (1989); **228**, 505 (1989).
- [27] J. F. Donoghue and C. Ramirez, *Phys. Lett. B* **234**, 361 (1990); S. Dawson and G. Valencia, *Nucl. Phys.* **B352**, 27 (1991).
- [28] G. Ecker, A. Pich, and E. de Rafael, *Nucl. Phys.* **B321**, 311 (1989); J. F. Donoghue, C. Ramirez, and G. Valencia, *Phys. Rev. D* **38**, 2195 (1988); **39**, 1947 (1989).
- [29] H. Lehmann, *Phys. Lett.* **41B**, 529 (1972); *Acta Phys. Austriaca Suppl.* **11**, 139 (1973); H. Lehmann and H. Trute, *Nucl. Phys.* **B52**, 280 (1973); G. Ecker and J. Honerkamp, *ibid.* **B52**, 211 (1973); see also H. Pagels, *Phys. Rep.* **16C**, 221 (1975).
- [30] O. Cheyette and M. K. Gaillard, *Phys. Lett. B* **197**, 205 (1987); T. Appelquist and C. Bernard, *Phys. Rev. D* **22**, 200 (1980); A. Longhitano, *Nucl. Phys.* **B188**, 118 (1981).
- [31] S. Dawson and S. D. Willenbrock, *Phys. Rev. D* **40**, 2880 (1989); *Phys. Rev. Lett.* **62**, 1232 (1989).
- [32] G. Valencia and S. D. Willenbrock, *Phys. Rev. D* **46**, 2247 (1992).
- [33] L. Durand, J. M. Johnson, and J. L. Lopez, *Phys. Rev. D* **45**, 3112 (1992).
- [34] W. J. Marciano and S. D. Willenbrock, *Phys. Rev. D* **37**, 2509 (1988).
- [35] S. D. Willenbrock and G. Valencia, *Phys. Rev. D* **42**, 853 (1990).
- [36] R. S. Chivukula, M. J. Dugan, and M. Golden, Report Nos. BUHEP-94-10, HUTP-94/4014, and hep-ph/9406281 (unpublished).
- [37] S. D. Willenbrock and G. Valencia, *Phys. Lett. B* **247**, 341 (1990).
- [38] S. Dawson and G. Valencia, *Nucl. Phys.* **B348**, 23 (1991).
- [39] G. 't Hooft and M. Veltman, *Nucl. Phys.* **B153**, 365 (1979).
- [40] D. Kominis and V. Koulovassilopoulos (unpublished).
- [41] A. Denner, U. Nierste, and R. Scharf, *Nucl. Phys.* **B367**, 637 (1991); U. Nierste, Diplomarbeit, Würzburg, 1991.

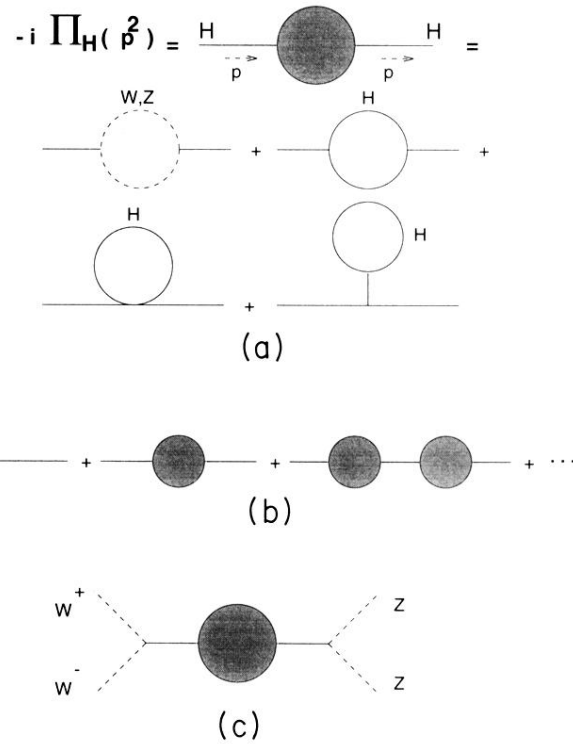


FIG. 2. (a) One-loop Higgs boson self-energy. (b) Sum of diagrams that replaces the propagator on the resonance region. (c) Higgs boson self-energy contribution to $w^+ w^- \rightarrow z z$. As explained in Sec. III B 1, for energies around the Higgs mass the resummed propagator is used from diagrams of Fig. 2(b).

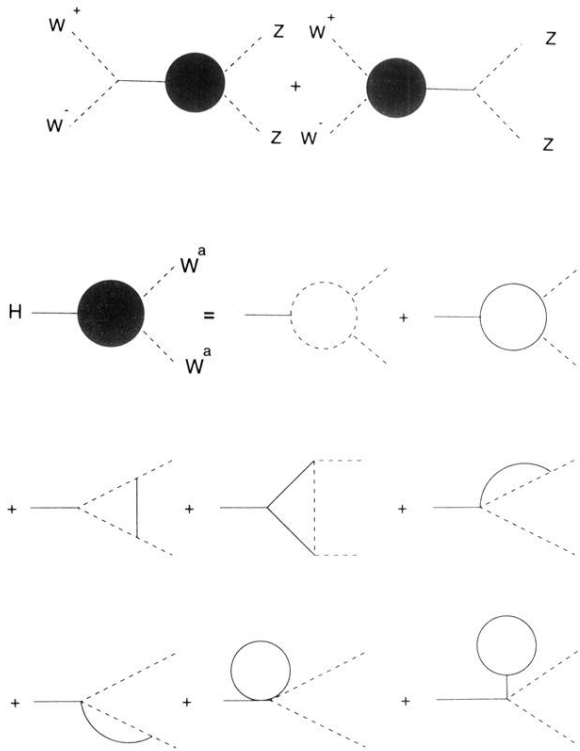


FIG. 4. The one-loop contribution to $w^+ w^- \rightarrow z z$ scattering amplitude through the $H w^a w^a$ vertex.